Research Article Adv. Mat. Lett. 2011, **2**(2), 142-147 ADVANCED MATERIALS Letters

www.vbripress.com, www.amlett.com, DOI: 10.5185/amlett.2011.1201 Published online by the VBRI press in 2011

Shape selective growth of ZnO nanostructures: spectral and electrochemical response

A.K. Srivastava[1*], M. Deepa[1], K.N. Sood[1], E. Erdem[2], R.-A.Eichel[2]

[1]*National Physical Laboratory, C.S.I.R., New Delhi 110012, India*
[2]*Technische Universität Darmstadt, D-64287 Darmstadt, Germany*

[*]Corresponding author. Tel: (+91) 11 45609308; Fax: (+91) 11 45609310; E-mail: aks@nplindia.ernet.in

Received: 1 Jan 2011, Revised: 23 Feb 2011 and Accepted: 28 Feb 2011

ABSTRACT

Novel growth morphologies of sharp needle-shaped tetrapods and coexistent tetrapods and nanowires of ZnO have been prepared by sublimation of pure Zn utilizing a simple solid – catalyst free - vapour mechanism at the temperatures of 950 and 1100 ºC, respectively. These striking differences in these microscopic objects, which evolved at two different process temperatures, were deduced from electron paramagnetic resonance and Raman spectra thereby revealing the role of microstructures, defects and oxygen vacancies in ZnO at lattice scale, which are receptive for luminescence, and electrochemical activity of this functional oxide.

Keywords: Nanostructures; oxides; electron microscopy; spectroscopy; electrochemical measurements.

A.K. Srivastava did Ph.D. at IISc Bangalore, (Metallurgy), M.Tech. at IIT, Kanpur (Materials Science), M.Sc. at IIT, Roorkee (Physics). He has collaborations with IISc Bangalore, BHU Varanasi, IIT Delhi, IIT Kanpur, University of Paris (France), University of Reims (France), Technical University Darmstadt (Germany), University of Arkansas (USA), University of Okayama (Japan) and POSTECH (South Korea). He has about 110 publications in highly reputed international journals like NanoLetters, Nanotechnology, Acta Materialia, Small, etc. and proceedings. He is DST (Govt. of India) BOYSCAST fellow. He is the recipient of INSA-fellowship under International exchange program. He has been awarded the Materials Research Society of India – Medal for the year 2011.

M. Deepa did Ph.D. at Delhi University (Chemistry). She carried out her major research work at National Physical Laboratory, New Delhi. Her research interests include syntheses of thin film nanostructures of transition metal oxides and conducting polymer composites by wet chemistry routes and probing their electrochemistry.

K.N. Sood is a Science Graduate from Delhi University and Post graduate from Panjab university, Chandigarh. His Main activity of work includes sample preparation for SEM, TEM and EDS and characterization of materials using SEM, EDS and TEM Techniques.

E. Erdem did PhD in Physics at University of Leipzig, M.Sc. in Physics at University of Leipzig and B.Sc. in Physics at University of Ankara. His main area of research includes, (i) Ferroelectric and ferromagnetic nano-crystalline materials (ii) Electron paramagnetic resonance spectroscopy, (iii) Raman and dielectric spectroscopy, and (iv) Nano-size effects, phase transitions, crystal field theory.

R.–A. Eichel did Ph.D. at Swiss Institute of Technology, Zurich, Switzerland, Diploma in Solid State Physics, University of Cologne, Germany and Post Doc at UC Berkley, USA. His research interests include characterization of defect-structure and investigation of nano-size effects in ferroelectric and multiferroic functional materials, molecular magnets, heterogeneous catalysts, phosphors, luminescent materials and semiconductors.

Introduction

Nanostructured materials are of great interest due to their various tunable microstructures, phase transformations and quantum confinements, a need for a gamut of engineering usage [**1-5**]. Among these nano – particles, wires, rings, combs, tetrapods of materials such as ZnO [**6-22**] and WO_3 [**23-28**] are very much in demand for future electronic, optical and optoelectronic nano-devices. For better ZnO-based emitters, it is of importance to fabricate ZnO arrays with sharp – tipped one dimensional structure. These nanostructures elastically accommodate a high level of strain allowing remarkable structural flexibility and very high strength up to several tens of Gigapascals (GPa) [**13, 14**]. Improved mechanical properties together with inherent slenderness (high aspect ratio) and its semiconductor characteristics predicts ideal proposition for the application of ZnO nanotips to atomic force microscope (AFM) probes, especially for measuring surfaces with higher degree of

undulation. Further, high hardness of ZnO would protect the probe tip from wear and damage during operation. Moreover various emission characteristics and shifting of luminescence bands can be attributed to the fine nanocrystalline structures leading to a large surface area and defects [**18, 19**].

In this study we report some of important findings pertaining to ZnO on its novel growth morphology and related spectroscopic, optical and electrochemical performance. The electrochemical charge insertion-extraction capability of ZnO has been reported and first time compared with that of WO_3, a well-established material for electrochemical applications. Moreover certain fundamental concerns on nanostructured ZnO pertaining to their preparation and correlating the ensuing microstructure with luminescence and electrochemical activity have been tackled to resolve queries of (i) effect of evaporation temperature on size and morphologies, (ii) consequences of microstructures on photoluminescence and redox behavior and (iii) correlation of magnetic resonance and Raman spectroscopic measurements with fine scale microstructures and potential applications. A qualitative relationship between process temperature, microstructure and oxygen vacancies, and defects has also been discussed.

Experimental

Material preparation

An economically viable high yield solid –vapour deposition technique was opted for preparation of ZnO nanostructures [**9**]. Unlike vapor-liquid-solid deposition, no catalyzing metal particles were used in the present case. Since it was a catalyst free synthesis no liquid phase was involved. In this process very high purity Zn granules in a quartz crucible covered with a thin quartz slide were placed in a horizontal muffle furnace. A Platinum/Rhodium thermocouple was located in the center of the furnace to measure its temperature. The experiments with two process temperatures of 950 ºC (referred as sample 1) and 1100 ºC (referred as sample 2) were carried out with the furnace-temperature stability of ±1 ºC. Oxidation of Zn vapors led to the nucleation and growth of ZnO nanostructures on the quartz slide. These experiments were conducted under ambient pressure.

Microstructural characterization

The crystallographic interpretations were performed by X-ray Diffractometer (XRD, Mini Flex II Desk Top X-ray Diffractometer) using Cu-K_α wavelength (λ=1.54059 Å) and scanning in 2θ range from 20 to 80º. Morphological features of white fluffy ZnO were characterised using a scanning electron microscope (SEM, LEO 440) equipped with an energy dispersive spectrometer (EDS, OXFORD LINK ISIS 300) and a cathodoluminescent detector. On an average three sets of samples were prepared at two different process temperatures (950 and 1100 ºC) and on each sample at least five different regions were characterized for imaging and composition analysis, using SEM and EDS. Consequently the data reported in the present work on each process temperature is an average value obtained after fifteen observations. A transmission electron microscope (TEM, JEOL JEM 200 CX) was used to carry out nano-scale imaging and corresponding reciprocal space analysis.

Photoluminescence and spectroscopy measurements

The sample loading for photoluminescence (PL) measurement was carried out in a standard holder of the following dimensions: ~2 cm diameter and 1 mm depth. The PL investigations were performed using a Perkin-Elmer LS–55 luminescence spectrophotometer having a standard Xe source with a filter that emits UV radiation. The emission of the samples was recorded at an excitation wavelength of 200 nm. The results were averaged out for ten times to reduce the background noise in the emission spectra. It must be mentioned here that during the excitation, second harmonics get generated due to the non-linear response of the material to the excitation wavelength. However, for recording the principal emission, an appropriate filter was employed to suppress the undesired response. Raman spectra were recorded on a Perkin-ELmer GX 2000 OPTICAL spectrophotometer. The source was Nd:YAG laser (λ = 1064 nm) and the detector was InGaAs. The resolution was 4 cm^{-1} and each sample was subjected to 1024 scans. The sample loading for Raman spectroscopy was carried out in a standard holder of 1 cm length and 0.5 cm diameter. The X band (9.5 GHz) electron paramagnetic resonance (EPR) measurements were carried out using ESP 300E spectrometer (Bruker), equipped with a rectangular TE112 resonator.

Electrochemical measurements

Homogeneous dispersions of ZnO powders (samples 1 and 2) of 0.25 M strength were prepared in ethanol and Poly(ethylene glycol) 400 mixed in a 1:1 volume ratio, by magnetic stirring at room temperature for thirty minutes. The solution was spin coated onto SnO_2:F coated glass substrates at 1000 rpm for 10 s. The films were thermally treated at 300 ^oC for two hours for organic burnout. Film thickness was determined using a Taylor Hobson Talystep; the thickness of the film formed from sample 1 was 1250 nm and the film derived from sample 2 was 1200 nm thick. Cyclic voltammetry (CV) was performed in a classical three-electrode electrochemical cell within ± 1.5 V, wherein ZnO acted as the working electrode, Ag/AgCl/KCl was employed as the reference electrode and a Pt rod was used as the auxiliary electrode. All electrochemical measurements were performed in an electrolyte solution of lithium triflate in γ-butyrolactone of one molar strength (1 M $LiCF_3SO_3$ - γBL).

Results and discussion

Structure and nano-scaled morphologies of ZnO

The X-ray diffractograms (XRD) recorded on different samples of ZnO revealed the formation of hexagonal – ZnO (wurtzite type; a = 0.32 , c = 0.52 nm) which was in close agreement to standard data (JCPDS file no. 21-1486). A representative XRD pattern of ZnO tetrapods samples elucidating the intense planes (hkil); $10\bar{1}0$, 0002, $10\bar{1}1$, $10\bar{1}2$, $11\bar{2}0$, $10\bar{1}3$, $20\bar{2}0$, $11\bar{2}2$ and $20\bar{2}2$ of interplanar spacings (d); 0.28, 0.26, 0.25, 0.19, 0.16, 0.15, 0.14, 0.138

and 0.124, respectively are indicated on the diffraction peaks (**Fig. 1**). A systematic microstructural imaging revealed that interesting morphologies of tetrapod – shaped ZnO were formed with a very high yield at the Zn evaporation temperature of 950 ºC (**Figs. 2a, b**). The tetrapods including the four legs of nano-needles posses, in general, overall dimensions of 3 to 15 μm. The curvature of the tips of nano needles (diameter: 20 to 150 nm) varied between 10 to 50 nm. The diameter of the nano needles was between 20 to 150 nm. Cathodoluminescence of these tetrapods has also been depicted as an inset of **Fig. 2(a)**. It has already been deduced [**14**] previously that such nucleation of ZnO with a growth in four different directions follows an octatwin model with preferred directions of [0001] and $[01\bar{1}0]$ in a hexagonal wurtzite crystal of ZnO. The tips of the tetrapod nanorods (legs) are sharp with blade like microstructure (**Fig. 2c**). The selected area electron diffraction pattern (SADP) recorded from the tetrapods (along $[01\bar{1}0]$ zone axis) has confirmed a single crystal growth of hexagonal structure with the lattice parameters, a = 3.25 Å and c = 5.21 Å, of ZnO (**inset of Fig. 2c**). Two diffraction spots on SADP marked as 1 and 2 are planes; $\bar{2}110$ and 0002 of hexagonal ZnO crystal structure.

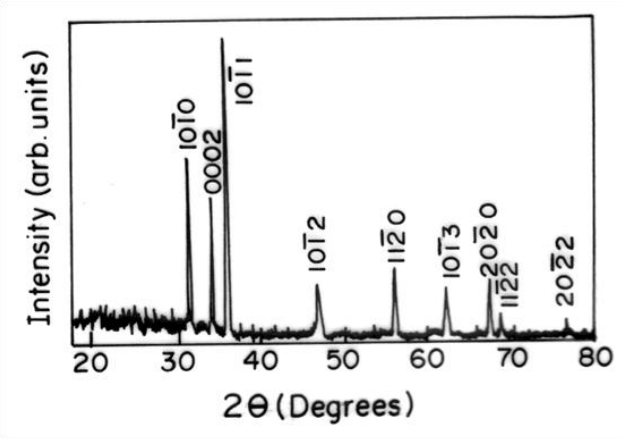

Fig. 1. XRD pattern of tetrapods showing the presence of important planes of ZnO-hexagonal crystal structure.

On increasing the evaporation temperature to 1100 ºC, the formation of tetrapod shapes of ZnO persists. However in the microstructure, a significant yield of long nanowires of few micro-scale in length grown at the tips of tetrapods has been delineated. The curvature of the tips of the nanowires varies from 10 to 50 nm (**Fig. 2d**). In general a ripple like microstructure is seen at the point of growth of nanowire from the end of tetrapod nanorods (**inset in Fig. 2d**). The evolution of ripple – like contrast at the junction-region may presumably be due to lattice strains during nucleation of nanowires. Furthermore, in both the cases (samples 1 and 2), only hexagonal – ZnO phase has been revealed by SADPs. We have not noticed any un-reacted Zn in the microstructure.

In our previous studies, it was established that the wire formation takes place in an oxygen deficient atmosphere while processing [**10**]. Furthermore, structural defects introduced as deficient sites act as nucleation points for further growth leading to a wire-encompassing microstructure. We have shown experimentally that on increasing the vacuum from 10^{-1} to 10^{-4} torr under thermal evaporation, the nanoparticles of ZnO, transform to a wire morphology [**10**]. However in present work as the temperature was increased, the growth of tetrapod nanostructures is accompanied by evolution of nanowires dangling at the tips of individual legs of tetrapods.

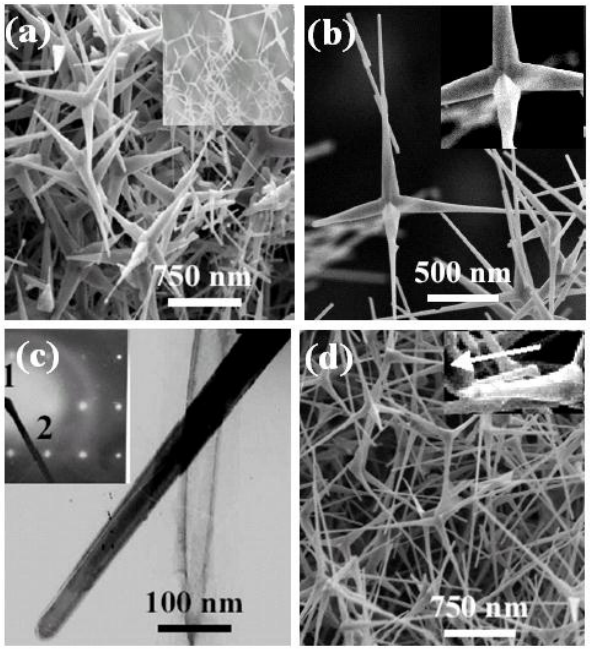

Fig. 2. Different microstructural features of tetrapods of sample 1 prepared at 950 °C (a, b, c). Inset in (a) shows cathodoluminescence. Inset in (b) shows a central-growth region of a tetrapod. Inset in (c) shows a SADP. Sample 2 prepared at 1100 °C shows (d) coexistent tetrapods and nanowires. Inset in (d) shows a ripple like growth.

Table 1. Details of process temperature, microstructure and composition of zinc oxide nanostructures prepared at 950 and 1100 °C.

Experiments	Evaporation temperature (°C)	Microstructure	Elements (at.%) Zn	O
Sample 1	950	Tetrapods with fine legs	52	48
Sample 2	1100	Coexistence of tetrapods and nanowires	62	38

The EDS measurements carried out on the specimens of tetrapods (950 ºC) and tetrapods with coexisting nanowires (1100 ºC) revealed the formation of zinc oxide with an average composition of $ZnO_{0.92}$ (Zn:O :: 52:48) and $ZnO_{0.61}$ (Zn:O :: 62:38), respectively. These compositions, in concurrence with our earlier investigations [**10**] affirm that the oxygen vacant sites are preferably the heterogeneous nucleants for the nanowire formation at 1100 ºC (sample 2); moreover the evolved nanowires are more deficient in oxygen, compared to the pristine tetrapod structures. **Table 1** lists the chemical composition and corresponding microstructures of sample 1 and 2 prepared at the evaporation temperatures of 950 and 1100 ºC, respectively. However it is worth mentioning that even on individual tetrapods (processed at 950 ^{o}C), the tips of their legs were more O deficient compared to central body of the tetrapod. In case of nanowires (i.e. the extended growth of legs of tetrapods seen at 1100 ^{o}C), on an average the composition of Zn and O was quite uniform throughout the

microstructure. Although **Table 1** illustrates an average value of different measurements, a set of typical EDS values recorded on three different microstructures are like, central body of a tetrapod: 53.71at% (Zn), 46.29at% (O); tip of a leg of a tetrapod: 57.30at% (Zn), 42.70at% (O); a nanowire: (60.86at% (Zn), 39.14 at% (O).

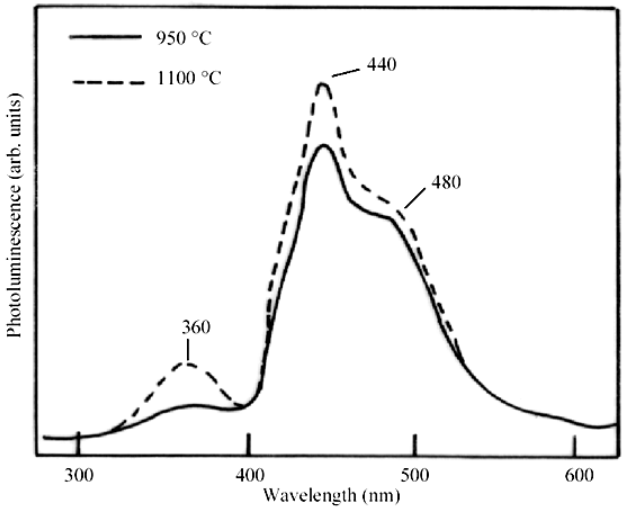

Fig. 3. Photoluminescence spectra of ZnO nanostructures prepared at 950 and 1100 °C.

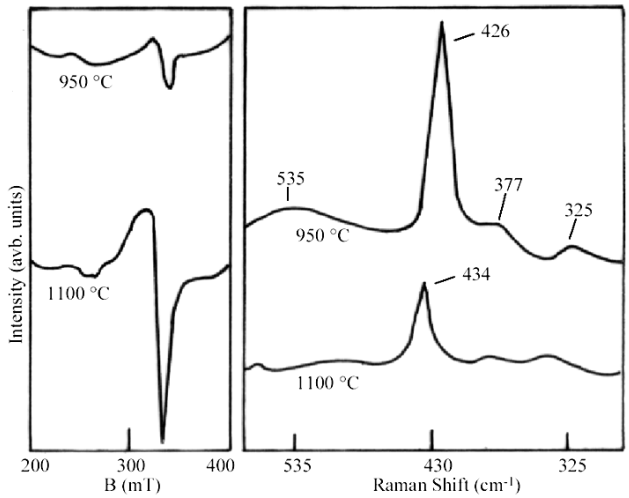

Fig. 4. (a) Experimental EPR spectra recorded at 10 K. (b) Room temperature Raman spectra, from samples prepared at 950 and 1100 °C.

Luminescence and spectroscopy observations

Implications of these nanostructures (**Fig. 2**) have been observed on room temperature photoluminescence spectra of tetrapods (950 ºC; sample 1) and tetrapods coexisting with nanowires (1100 ºC; sample 2) upon photoexcitation at 200 nm (**Fig. 3**). Both samples reveal broad band PL emissions centered around 360, 440 and 480 nm. However, sample 2 depicts emergence of additional shoulders around 415 and 520 nm. In a detailed investigations, mechanism for the evolution of different emission bands are described [**10, 15**]. The UV emission at around 360 nm is due to excitonic recombination leading to near-band-edge (NBE) emission of ZnO, which increased markedly in sample 2, indicating improved nanocrystallinity at higher temperatures. However the blue emission at approximately 440 and 480 nm can be attributed to intrinsic defects, particularly interstitial zinc (Zn_i), evolved with deviation in stoichiometry of ZnO. Since sample 2 is more deviated ($ZnO_{0.61}$) than sample 1 ($ZnO_{0.92}$) from stoichiometric ZnO, indicates higher defects leading to a higher recombination rate of photogenerated charge carriers. Moreover in sample 2, the grain size/diameter of the tips of nano-needles decreased, resulting in higher surface-to-volume ratio leading to an overall increase in surface trapping process, hence higher PL intensity. The shoulder around 415 nm corresponds to violet emission, which is probably caused due to radiative transitions between radiative defects levels (R_d), related to interface traps existing between the grain boundaries of ZnO and the valence band. The shoulder at around 520 nm corresponds to green emission, which is referred to as deep-level emission, is attributed to the recombination of electrons trapped in singly ionized oxygen vacancies O^- with holes.

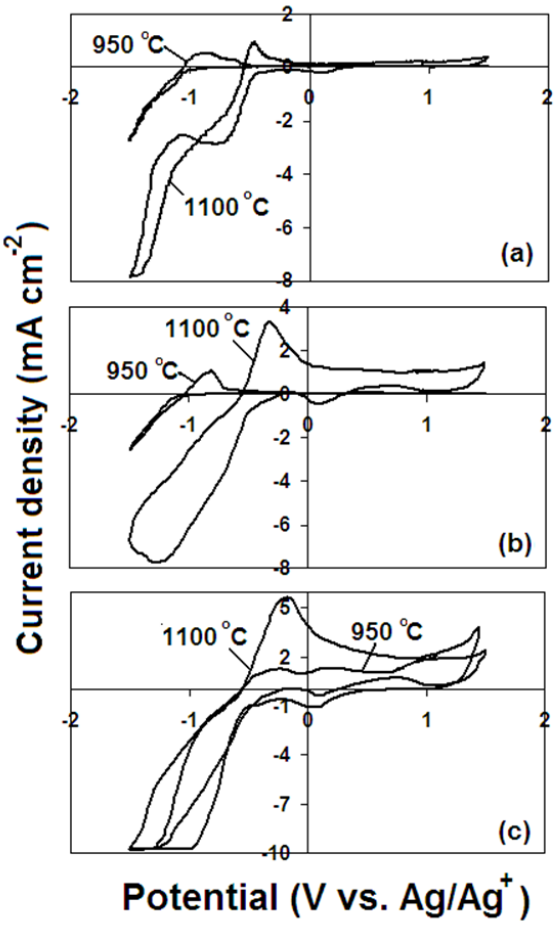

Fig. 5. Cyclic voltammograms of ZnO samples, prepared at 950 and 1100°C, recorded at sweep rates of (a) 5, (b) 50 and (c) 100 mV s^{-1} in a 1 M $LiCF_3SO_3$-γBL electrolyte.

The observations in PL spectra are corroborated with the findings of EPR and Raman spectroscopy to discern the possible means (oxygen vacancies and surface to volume ratio) or defects due to differing nano-morphologies of these useful microscopic novel objects. X-band (microwave frequency, 9.5 GHz) EPR spectra at liquid He

(temperature: 10 K) for both the samples 1 and 2, revealed the splitting at about 330 mT (**Fig. 4a**). The corresponding g-factor observed from simulation was ~ 1.95. It is worth mentioning that these samples were initially run at room temperature, but no EPR signal was acquired. A comparison of the EPR spectra for the two zinc oxide samples with their corresponding stoichiometry, shows that sample 2 (tetrapods with nanowires, low oxygen-content, $ZnO_{0.61}$) produces a strong EPR signal whereas sample 1 (tetrapods, high oxygen-content, $ZnO_{0.92}$) gives rise to a weak EPR signal. These results support the idea that the nanowired ZnO (tetrapods) contain significant proportion of oxygen vacancies, which effectively leads to strong intensities of blue luminescence (**Fig. 3**). In this regard, the more number of dangling bonds associated with $ZnO_{0.61}$ may attribute to intense peak at EPR signal. **Fig. 3b** shows room temperature Raman spectra of these samples between wave numbers at 350 to 550 cm^{-1}. In general, being hexagonal (Wurtzite-$P6_3mc$) ZnO, the low intensity peaks at around 325, 377 and 535 cm^{-1} (in both the samples) arise due to different phonon modes of E_2: low and high frequency, A_1: TO and LO and E_1: TO and LO, symmetric and asymmetric [**12**]. In this series, the high frequency E_2 mode (highly intense) is clearly visible at 426 cm^{-1} (sample 1) and at 434 cm^{-1} (sample 2). It is noteworthy that the Raman shift of 2LO phonons of ZnO tetrapods coexisting with nanowires is located at 434 cm^{-1}, and this exhibits an upshift of the 2LO mode by about 8 cm^{-1}, compared to the 2LO mode observed from ZnO tetrapods at 426 cm^{-1}. Moreover the peak at 434 cm^{-1} is less intense compared to a similar phonon peak at 426 cm^{-1}. This phenomenon may be explained on the basis that the ultrafine nanowires (sample 2) have much higher surface area and more surface defects including oxygen-vacancies than the tetrapods alone (sample 1). This could have induced the weakening of the phonons and shift of the 2LO modes.

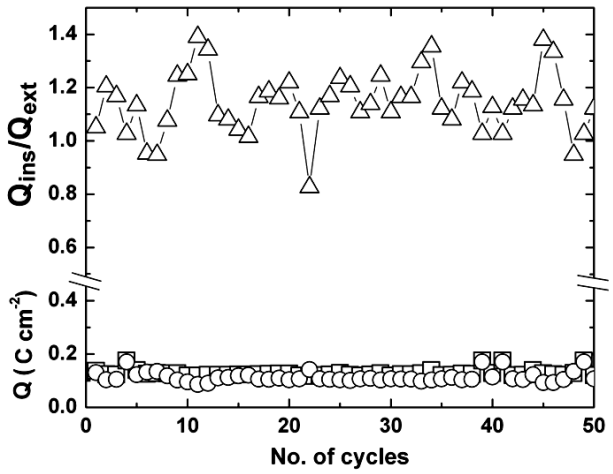

Fig. 6. Variation of charge intercalated (□) and deintercalated (○) and the ratio of inserted to extracted charge (△) as a function of cycling in sample 2 in a 1 M $LiCF_3SO_3$-γBL electrolyte.

Electrochemical response

The electrochemical charge insertion-extraction capacity of ZnO is of paramount significance for employing the material as a reversible ion intercalation-deintercalation electrode in solar and solid-state electrochemical cells. Cyclic voltammograms recorded for the samples at different scan speeds in the range of 5 - 100 mV s^{-1} are displayed in **Fig. 5**. The cathodic process involved reduction of ZnO by insertion of electrons and the charge compensating lithium ions from the electrolyte and the anodic wave signals the oxidation of the oxide by expulsion of electrons and cations. The current density peak in the cathodic and anodic waves gives a rough estimate of the electrochemical activity of the electrode. At a fixed scan rate of 100 mV s^{-1}, the larger magnitude of the anodic peak current density (5.6 mA cm^{-2}) observed for sample 2 as compared to a value of 1.3 mA cm^{-2} from sample 1 is indicative of the superior redox activity of the former and this trend was observed at all other sweep rates as well. At a high scan rate of 100 mV s^{-1}, the saturation in the current (for sample 2) is due to the rapid depletion of ionic current, as both high scan rate and the superior ability of this material to uptake ions permits a swift attainment of steady state current value. Further, a charge storage capacity (a measure of the quanta of ions the oxide can uptake per unit active area per unit thickness and obtained by integration of the area under the i vs. t curves in the cathodic cycle) of 266 C cm^{-3} achieved for sample 2 is again higher than a value of 192 C cm^{-3} observed for its counterpart (sample 1). Further, this value (for sample 1) is comparable to the charge storage capacity of 270 C cm^{-3}, which we observed for a conventional ion-intercalation electrochromic material like tungsten oxide [**28**]. Moreover the ratio of inserted charge to extracted charge (Q_{ins}/Q_{ext}) obtained over 50 cycles of intercalation and deintercalation is in the range of 1.0 - 1.4 for sample 2, whereas for its analogue (sample 1), this ratio varies between 2.6 - 2.8. The variation in inserted and extracted charge and Q_{ins}/Q_{ext} as a function of cycling for sample 2 (ZnO, 1100 ^oC) is shown in **Fig. 6**. Since the ratio lies in the range of 1.0-1.4, it is obvious that some lithium ions are irreversibly trapped in the material during cycling. A possible electrochemically reversible reaction may be understood as:

$$ZnO + xLi^+ + xe^- \leftrightarrows Li_xZnO \quad \text{---------- (1)}$$

Similar intercalation-deintercalation studies have been earlier observed for ZnO films fabricated by pulsed laser deposition [**27, 28**] and for ZnO powders prepared by ball milling [**28**]. Such a high value of the Q_{ins}/Q_{ext} ratio for the sample 1 indicates that the material is not efficient at deintercalation, as the material does not allow a reversible ion insertion–extraction process. The Q_{ins}/Q_{ext} ratio is close to unity for sample 2 and this is indicative of the superior and quasi-reversibility (of charges) shown by the material. It is well-known that a high/optimized concentration of oxygen vacancies in transition metal oxides improves their ion storage capacity. These observations indicate that the more substoichiometric $ZnO_{0.61}$ constituted of tetrapods and nanowires is a promising electrode material for practical electrochemical applications.

Conclusion

Controllable anion deficiency in zinc oxide nanostructures has been accomplished by means of two unique morphologies: one comprising ZnO tetrapods only and the

other encompassing tetrapods and nanowires. The influence of oxygen vacancies and variant nanoobjects is reflected in their optical, luminescence response and electrochemical activity. Such a comprehensive evaluation of ZnO nanostructures in view of their practical utility in different important applications has been reported first time. Queries pertaining to luminescence, its reasons associated to oxygen vacancies and the dimensions/geometry of nanostructures have been experimentally understood with the assistance of advanced spectroscopic investigations. A vital manifestation of this work is that by altering the shape-selective growth of zinc oxide, the optical, chemical and electrochemical properties can be tuned, leading to the possibility of fabricating smart nano-devices.

Acknowledgement

We thank Dr. D. Gupta and Dr. H. Kishan for Raman spectroscopy and XRD measurements, respectively. Mr. J.S.Tawale and Dr. N. Bahadur are acknowledged for many useful discussions. Director, NPL is acknowledged for providing necessary experimental facilities.

References

1. Gleiter, H. *Acta Mater*. **2000**, *48*, 1. **DOI:** 10.1016/S1359-6454(99)00285-2
2. H.S. Nalwa, *Handbook of Nanostructured Materials and Nanotechnology*, Academic Press Publishing, Tokyo, **2000**.
3. Carlier, F.; Benrezzak, S.; Cahuzac, Ph.; Kébaïli, N.; Masson, A.; Srivastava, A.K.; Colliex, C.; Bréchignac, C. Nano Lett**.** **2006**, 6, 1875. **DOI:** 10.1021/nl060781n
4. Pan, Z.W.; Dai, Z.R.; Wang, Z.L. *Science* **2001,** *291*, 1947. **DOI:**10.1126/science.1058120
5. Peng, X.; Mania, L.; Yang, W.; Wickham, J.; Scher, E.; Kadvanich, A.; Alivisatos, A.P. *Nature* **2000,** *404***,** 59. **DOI:** 10.1038/35003535
6. Wang, Z.L. *J. Phy: Condens. Matter*. **2004,** *R829***,** 16. **DOI:** 10.1088/0953-8984/16/25/R01
7. Kong, X.Y.; Ding, Y.; Yang, R.; Wang, Z.L. *Science* **2004**, *303*, 1348. **DOI:** 10.1126/science.1092356
8. Roy, V.A.L.; Djurisic, A.B.; Chan, W.K.; Gao, J.; Lui, H.F.; Surya, C. *Appl. Phys. Lett*. **2003**, *83*, 141. **DOI:** 10.1063/1.1589184
9. Srivastava, A.K.; Sood, K.N.; Lal, K.; Kishore, R. *Patent filed ref. no. 0773DEL2005* dated 31st March, **2005**.
10. Srivastava, A.K.; Gupta, N.; Lal, K.; Sood, K.N.; Kishore, R. *J. Nanosci. Nanotech*. **2007**, *7*, 1941. **DOI:** 10.1166/jnn.2007.745
11. Srivastava, A.K.; Kishore, R. *Nano Lett*. **2005**, *5*, 1029. **DOI:** 10.1021/nl050788p
12. Calleja, J.M.; Cardona, M. *Phys. Rev*. B **1977**, *16*, 3753. **DOI:** 10.1103/PhysRevB.16.3753
13. Gordon, J.E. *The New Science of Strong Materials*. London: Pitman, **1976**.
14. Iwanaga, H.; Fujii, M.; Ichihara, M.; Takeuchi, S. *J. Cryst. Growth* **1994**, *141*, 234. **DOI:** 10.1016/0022-0248(94)90116-3
15. Srivastava, A.K.; Deepa, M.; Bahadur, N.; Goyat, M.S. *Mater. Chem. Phys.* **2009**, *114*, 194. **DOI:** 10.1016/j.matchemphys.2008.09.005
16. Dijken, A.V.; Meulenkamp, E.A.; Vanmaekelbergh, D.; Meijerink, A. *J. Luminescence* **2000**, *87-89*, 454. **DOI:** 10.1016/S0022-2313(99)00482-2
17. Wu, C.; Qiao, X.; Luo, L.; Li, H. *Mater. Res. Bull*. **2008**, *43*, 1883. **DOI:** 10.1016/j.materresbull.2007.07.025
18. Snure, M.; Tiwari, A. *J. Appl. Phys.* 2008, *104*, 073707. **DOI:** 10.1063/1.2988131
19. Snure, M.; Tiwari, A. *J. Nanosci. Nano Tech.* **2007**, *7*, 481. **DOI:** 10.1166/jnn.2007.139
20. Rai, R. *Adv. Mat. Lett.* **2010**, *1*, 55. **DOI:** 10.5185/amlett.2010.3101
21. Kiri, P.; Hyett, G.; Binions, R. *Adv. Mat. Lett.* **2010**, *1*, 86. **DOI:** 10.5185/amlett.2010.8147
22. Srivastava, A.K. *Mater. Lett.* **2008**, *62*, 4296. **DOI:** 10.1016/j.matlet.2008.07.09
23. Srivastava, A.K.; Agnihotry, S.A.; Deepa, M. *Thin Solid Films* **2006**, *515*, 1419. **DOI:** 10.1016/j.tsf.2006.03.055
24. Deepa, M.; Srivastava, A.K.; Sood, K.N.; Agnihotry, S.A. *Nanotechnology* **2006**, *17*, 2625. **DOI:** 10.1088/0957-4484/17/10/030
25. Deepa, M.; Srivastava, A.K.; Agnihotry, S.A. *Acta Mater*. **2006**, *54*, 4583. **DOI:** 10.1016/j.actamat.2006.05.044
26. Deepa, M.; Srivastava, A.K.; Agnihotry, S.A. *J. Phys.D: Appl. Phys.* 2006, 39**,** 1885.
27. **DOI:** 10.1088/0022-3727/39/9/025
28. Fu, Z.W.; Zhang, L.N.; Qin, Q.Z.; Zhang, Y.H.; Zeng, X.K.; Cheng, H.; Huang, R.B.; Zheng, L.S. *J. Phys. Chem. A* **2000**, *104*, 2980. **DOI:** 10.1021/jp993834g
29. Belliard, F.; Connor, P.A.; Irvine, J.T.S. *Solid State Ionics* **2000**, *135*, 163. **DOI:** 10.1016/S0167-2738(00)00296-4

